

1 **Supplementary Material for *Online Measurement of Gas-***  
2 ***Phase Nitrated Phenols Utilizing CI-LToF-MS: Primary***  
3 ***Sources and Secondary Formation***

4 Kai Song<sup>1,2</sup>, Song Guo<sup>1,2\*</sup>, Haichao Wang<sup>3</sup>, Ying Yu<sup>1</sup>, Hui Wang<sup>1</sup>, Rongzhi Tang<sup>1</sup>,  
5 Shiyong Xia<sup>4</sup>, Yuanzheng Gong<sup>1</sup>, Zichao Wan<sup>1</sup>, Daqi Lv<sup>1</sup>, Rui Tan<sup>1</sup>, Wenfei Zhu<sup>1</sup>,  
6 Ruizhe Shen<sup>1</sup>, Xin Li<sup>1</sup>, Xuena Yu<sup>1</sup>, Shiyi Chen<sup>1</sup>, Liming Zeng<sup>1</sup>, Xiaofeng Huang<sup>4</sup>

7  
8 <sup>1</sup> State Key Joint Laboratory of Environmental Simulation and Pollution Control,  
9 International Joint Laboratory for Regional Pollution Control, Ministry of Education  
10 (IJRC), College of Environmental Sciences and Engineering, *Beijing*, 100871, China

11 <sup>2</sup> Collaborative Innovation Center of Atmospheric Environment and Equipment  
12 Technology, Nanjing University of Information Science & Technology, *Nanjing*  
13 210044, China P. R.

14 <sup>3</sup> School of Atmospheric Sciences, Sun Yat-sen University, *Zhuhai*, 519082, China.

15 <sup>4</sup> Key Laboratory for Urban Habitat Environmental Science and Technology, School of  
16 Environment and Energy, Peking University Shenzhen Graduate School, *Shenzhen*,  
17 518055, China.

18 \* Correspondence to: S. Guo: [songguo@pku.edu.cn](mailto:songguo@pku.edu.cn)

19

20 **Figures**

21 **Figure S1.** Chemical structures and high-resolution peak fits of reagent ions and  
22 nitrated phenols (NPs) investigated in this study.

23 **Figure S2.** (a) Background ions and ions detected during the calibration period (local  
24 time); (b) Calibration line of ions ( $y$ ) and the standard gas-phase concentration of  
25 nitrophenol ( $x$ ).

26 **Figure S3.** The measured concentration of nitrated phenols and their secondary  
27 formation simulation by the box model.

28 **Figure S4.** Air quality and meteorology conditions during the sampling period in  
29 Beijing: time series of (a) wind speed, (b) RH, (c) PM<sub>2.5</sub>, (d) NO<sub>y</sub> and (e) CO from Dec  
30 1 to Dec 31, 2018.

31 **Figure S5.** Consensus maps of brunet, KL, offset, lee, nsNMF and snmf/l algorithms  
32 in NMF. The consensus approach was used to estimate the proper method and cluster  
33 method of simulation. The color of the consensus map indicated the coefficient and an  
34 ideal consensus map was a color-coded heat map in which red blocks along the diagonal  
35 on a blue background (Monti et al., 2003; Simpson et al., 2010). KL approach was the  
36 optimal one.

37 **Figure S6.** NMF rank survey of factors 3 to 7. The cophenetic coefficient and RSS  
38 curves were used for the judgment of factor numbers. The first decreasing cophenetic  
39 value (Brunet et al., 2004) and an inflection point of the RSS curve (Hutchins et al.,  
40 2008) was the optimal factor number, that was, four factors in this study.

41 **Figure S7.** Diurnal profiles of coal combustion (a), biomass burning (b), industry (c)  
42 and vehicle exhaust (d) sources. Coal combustion and biomass burning displayed a  
43 nighttime peak while the source of vehicle exhaust showed peaks at rush hour which  
44 were evidence of the NMF source apportionment.

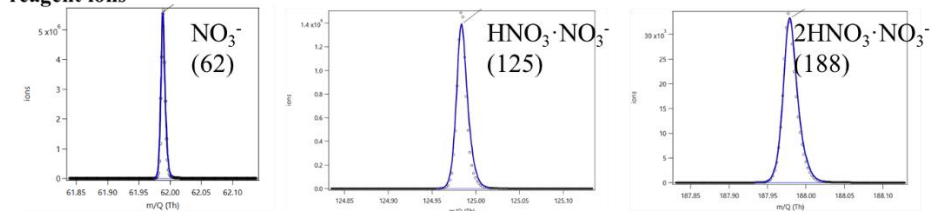
45 **Figure S8.** Source profile from the PMF model. (a) Source profile of PMF results. SO<sub>2</sub>,  
46 chloromethane, aromatics and 1,3-butadiene as the markers of coal combustion,  
47 biomass burning, industry and vehicle exhaust sources. (b) Contribution of primary  
48 emission (in blue borderline) and second formation (in red borderline) of NPs.

49

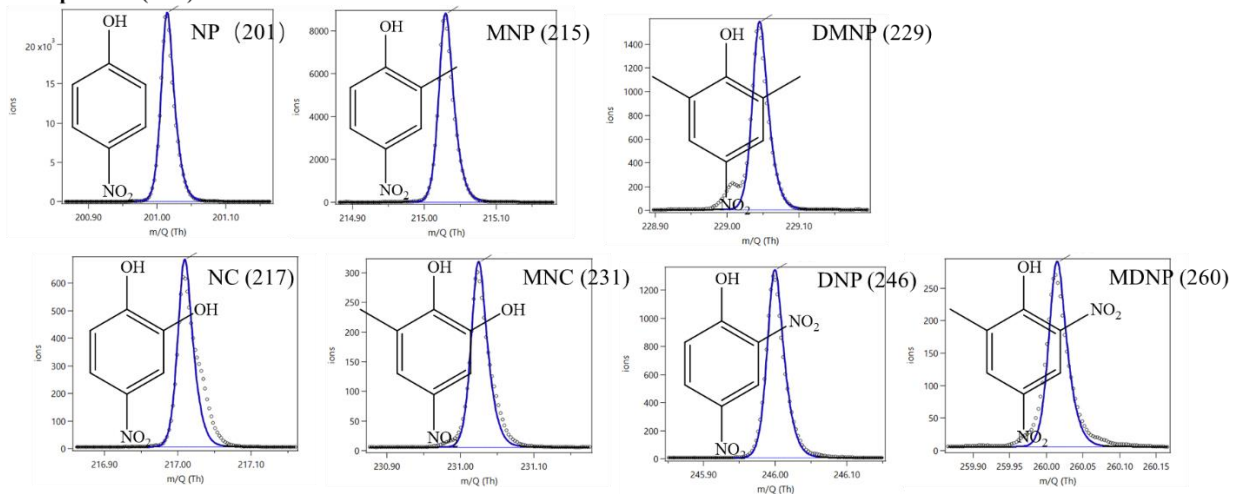
50

51

**reagent ions**



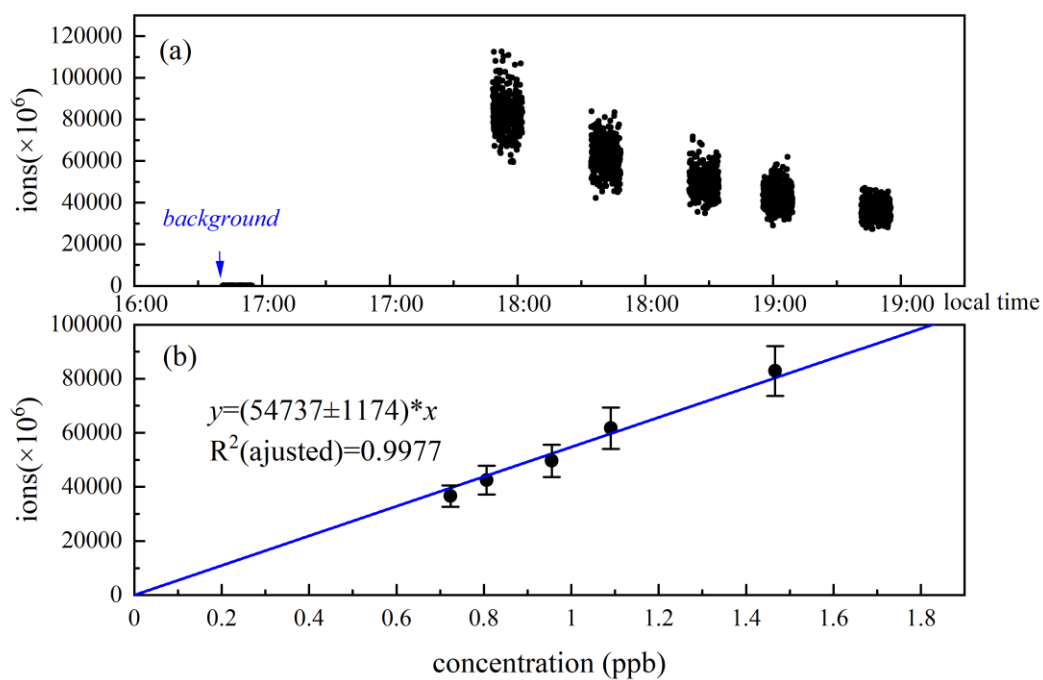
**nitrophenols (NPs)**



52

53 Figure S1. Chemical structures and high-resolution peak fits of reagent ions and nitrated  
54 phenols (NPs) investigated in this study.

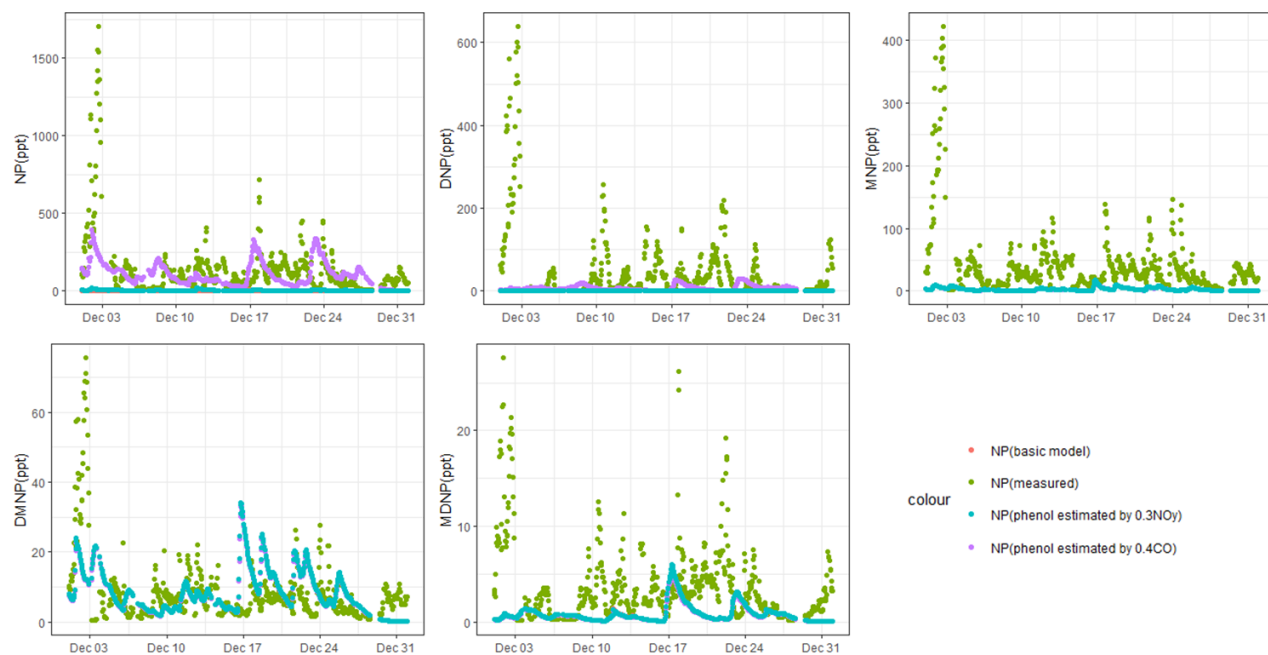
55



56

57 Figure S2. (a) Background ions and ions detected during the calibration period (local  
 58 time); (b) Calibration line of ions ( $y$ ) and the standard gas-phase concentration of  
 59 nitrophenol ( $x$ ).

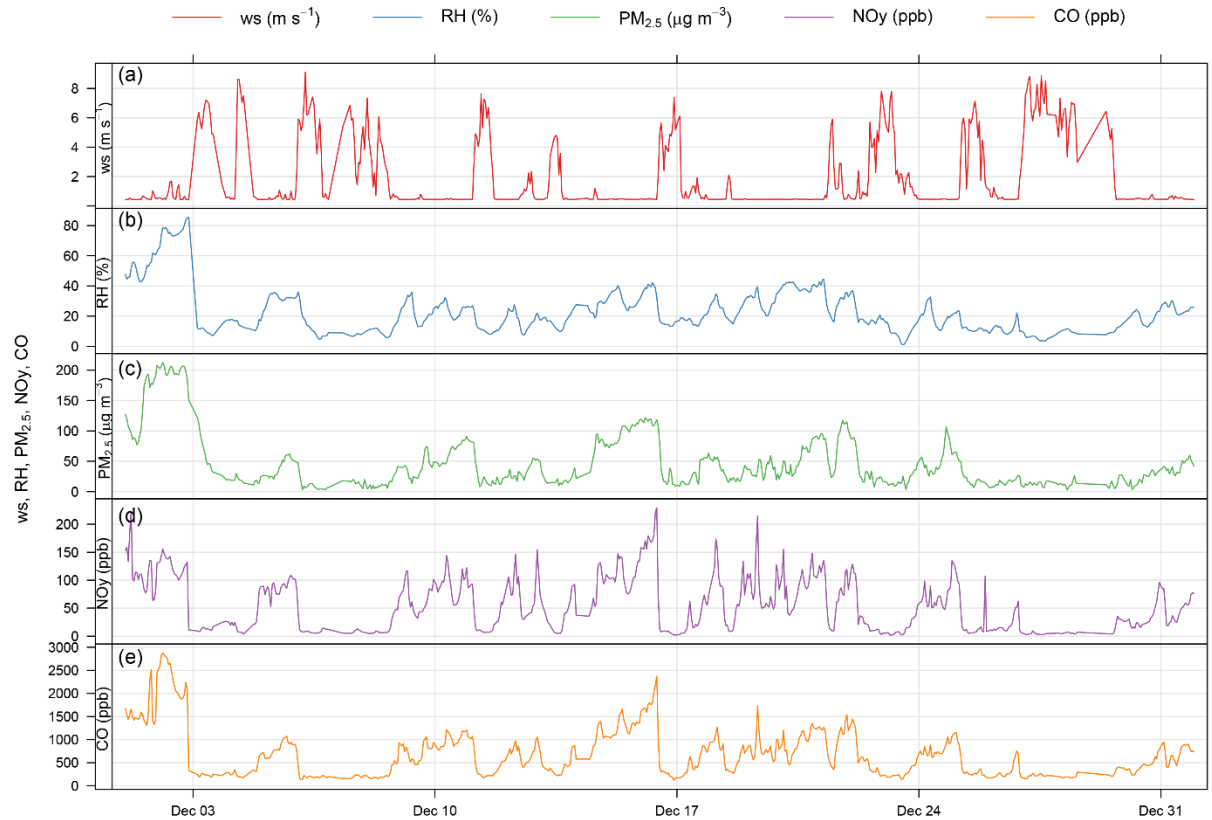
60



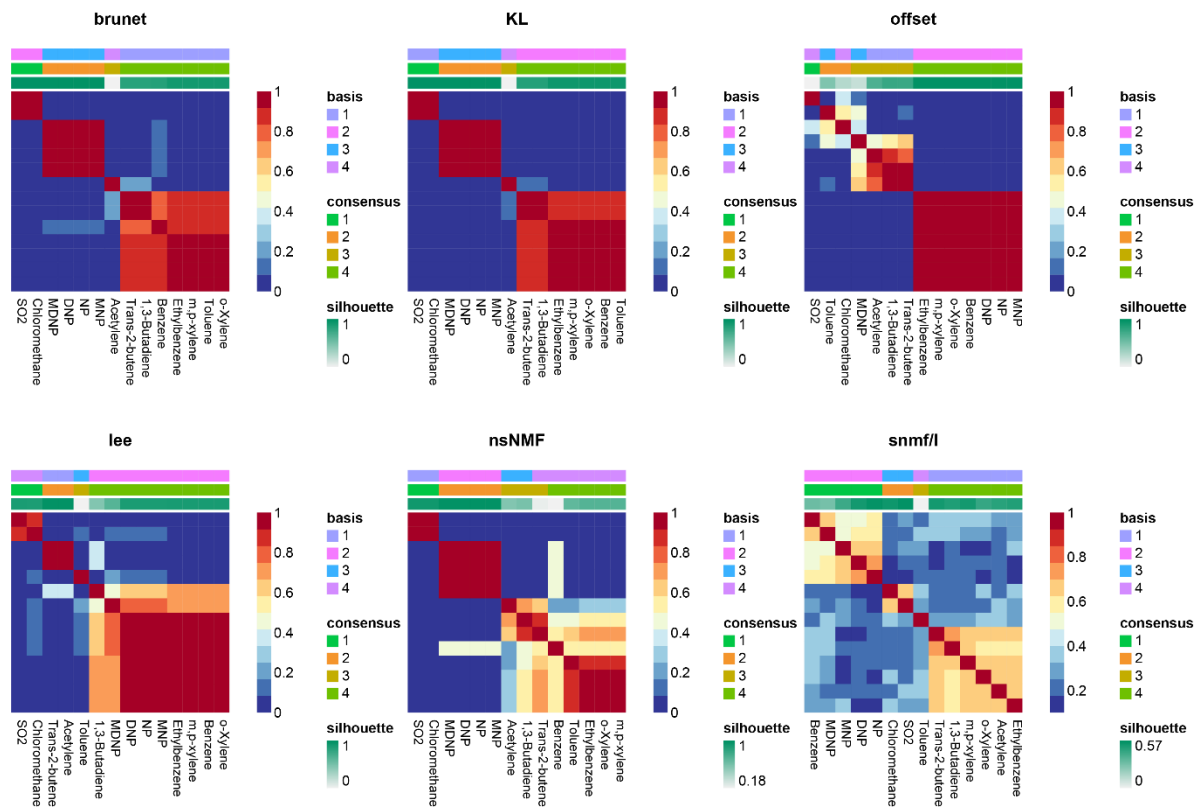
61

62 Figure S3. The measured concentration of nitrated phenols and their secondary  
 63 formation simulation by the box model.

64



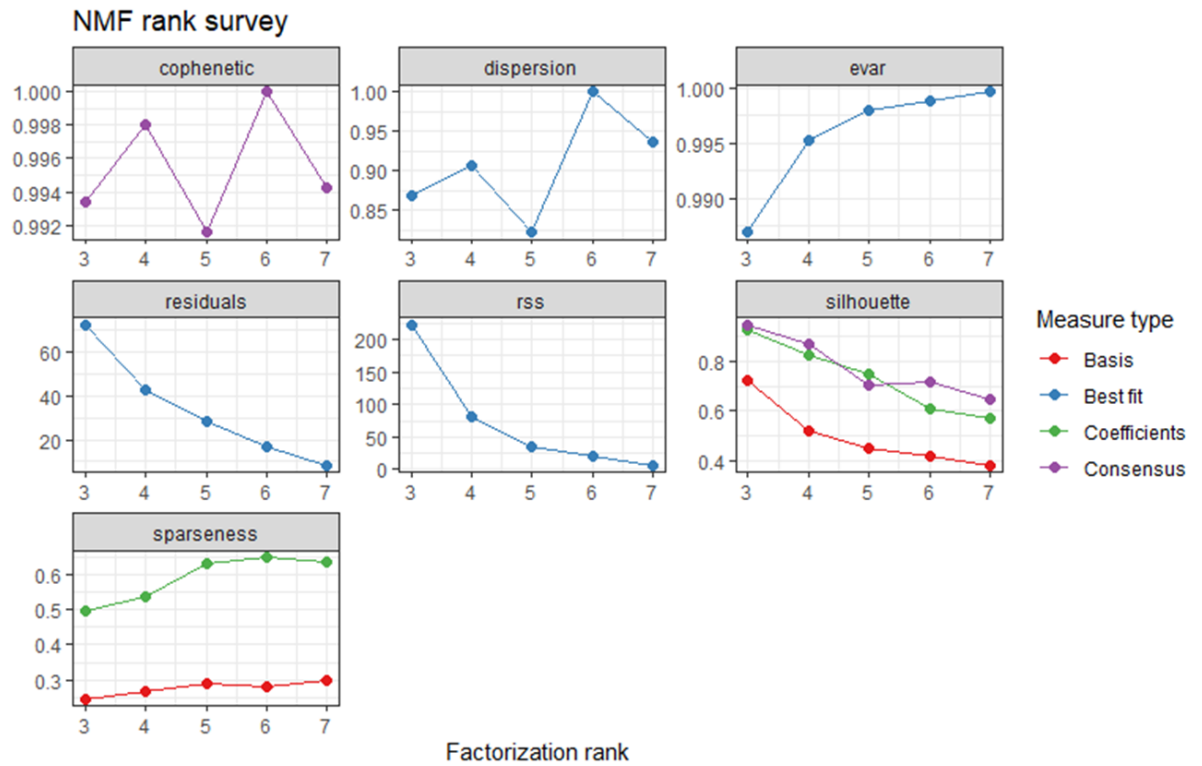
65  
 66 Figure S4. Air quality and meteorology conditions during the sampling period in  
 67 Beijing: time series of (a) wind speed, (b) RH, (c) PM<sub>2.5</sub>, (d) NO<sub>y</sub> and (e) CO from Dec  
 68 1 to Dec 31, 2018.  
 69



70

71 Figure S5. Consensus maps of brunet, KL, offset, lee, nsNMF and snmf/l algorithms in  
 72 NMF. The consensus approach was used to estimate the proper method and cluster  
 73 method of simulation. The color of the consensus map indicated the coefficient and an  
 74 ideal consensus map was a color-coded heat map in which red blocks along the diagonal  
 75 on a blue background (Monti et al., 2003; Simpson et al., 2010). KL approach was the  
 76 optimal one.

77



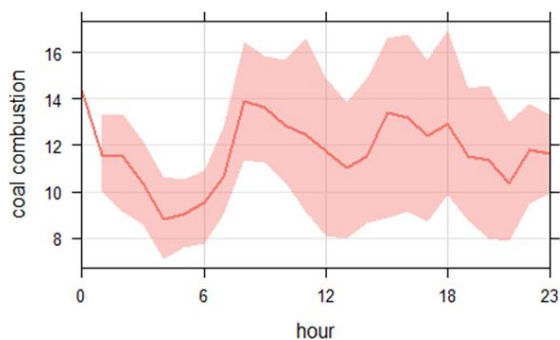
78

79 Figure S6. NMF rank survey of factors 3 to 7. The cophenetic coefficient and RSS  
 80 curves were used for the judgment of factor numbers. The first decreasing cophenetic  
 81 value (Brunet et al., 2004) and an inflection point of the RSS curve (Hutchins et al.,  
 82 2008) was the optimal factor number, that was, four factors in this study.

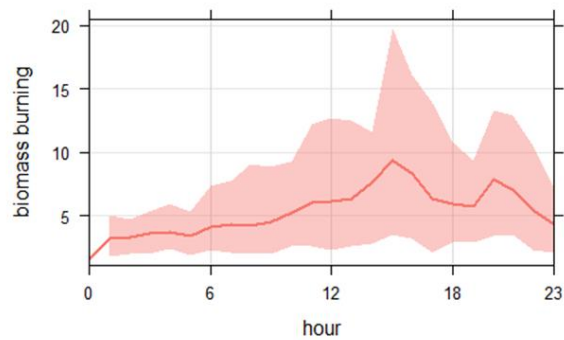
83



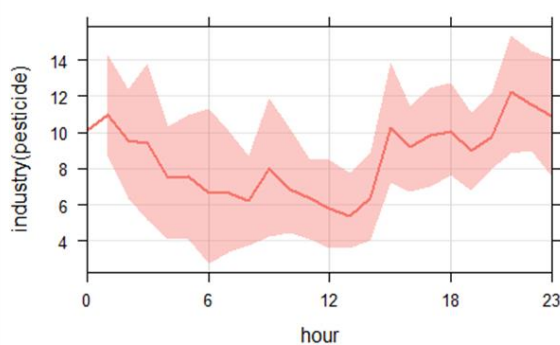
(a) coal combustion



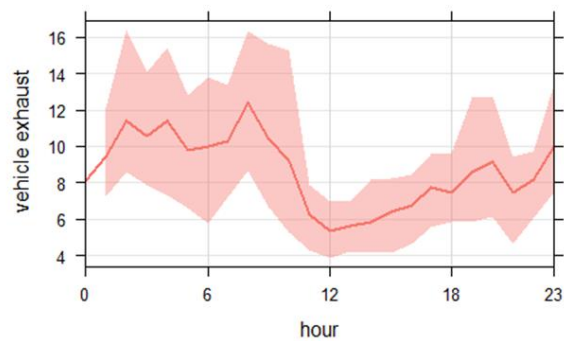
(b) biomass burning



(c) industry



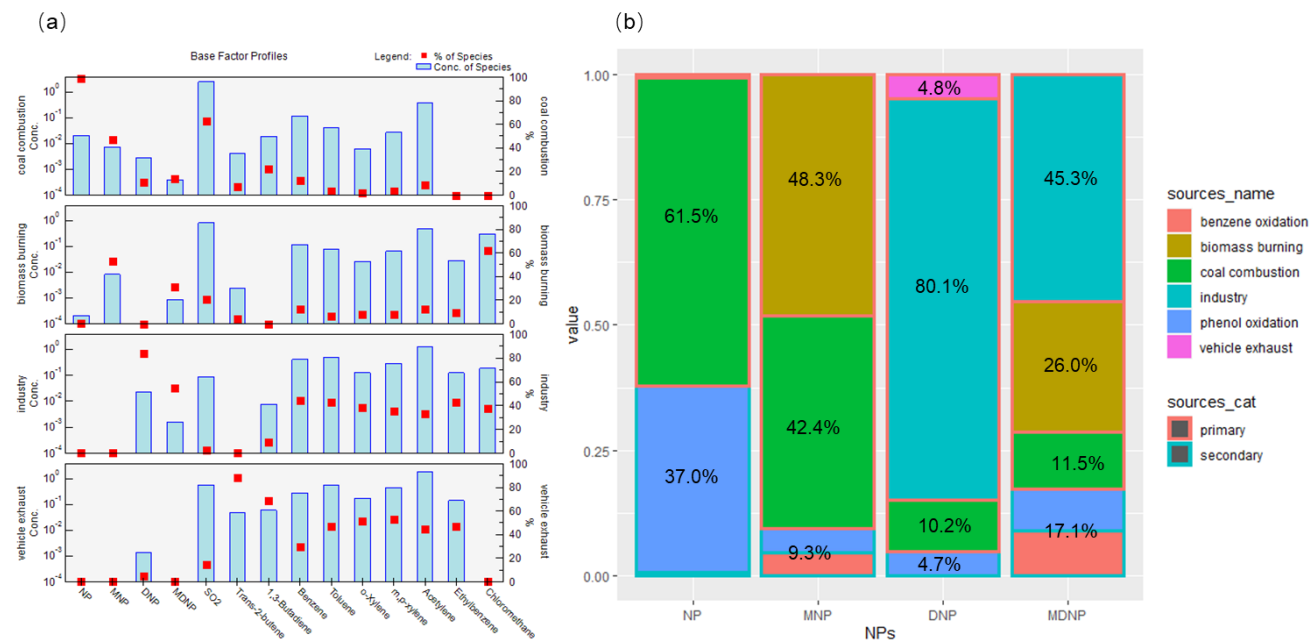
(d) vehicle exhaust



84

85 Figure S7. Diurnal profiles of coal combustion (a), biomass burning (b), industry (c)  
86 and vehicle exhaust (d) sources. Coal combustion and biomass burning displayed a  
87 nighttime peak while the source of vehicle exhaust showed peaks at rush hour which  
88 were evidence of the NMF source apportionment.

89



90

91 Figure S8. Source profile from the PMF model. (a) Source profile of PMF results. SO<sub>2</sub>,

92 chloromethane, aromatics and 1,3-butadiene as the markers of coal combustion,

93 biomass burning, industry and vehicle exhaust sources. (b) Contribution of primary

94 emission (in blue borderline) and second formation (in red borderline) of NPs.

95

96 **References**

- 97 Brunet, J. P., Tamayo, P., Golub, T. R. and Mesirov, J. P.: Metagenes and molecular  
98 pattern discovery using matrix factorization, Proc. Natl. Acad. Sci. U. S. A.,  
99 doi:10.1073/pnas.0308531101, 2004.
- 100 Hutchins, L. N., Murphy, S. M., Singh, P. and Graber, J. H.: Position-dependent motif  
101 characterization using non-negative matrix factorization, Bioinformatics,  
102 doi:10.1093/bioinformatics/btn526, 2008.
- 103 Monti, S., Tamayo, P., Mesirov, J. and Golub, T.: Consensus clustering: A resampling-  
104 based method for class discovery and visualization of gene expression microarray data,  
105 Mach. Learn., doi:10.1023/A:1023949509487, 2003.
- 106 Simpson, T. I., Armstrong, J. D. and Jarman, A. P.: Merged consensus clustering to  
107 assess and improve class discovery with microarray data, BMC Bioinformatics,  
108 doi:10.1186/1471-2105-11-590, 2010.
- 109